Experimental methods using force application of a single boom for a 500-m²-class solar sail

Martin Richter[1]
Institute of Lightweight Systems (formerly Institute of Composite Structures and Adaptive Systems), DLR German Aerospace Center, Braunschweig, 38108, Germany

Juan M. Fernandez[2]
NASA Langley Research Center, Hampton, VA, 23681, USA

and

Marco Straubel[3] ,Martin E. Zander[4]
Institute of Lightweight Systems (formerly Institute of Composite Structures and Adaptive Systems), DLR German Aerospace Center, Braunschweig, 38108, Germany

Joshua E. Salazar[5], Matthew K. Chamberlain[6]
NASA Langley Research Center, Hampton, VA, 23681, USA

Solar sailing missions rely on deployable systems for large area-to-mass ratios once in space, while still being small enough for launcher envelopes in the stowed configuration. Many of these deployable systems feature booms that are flattened and subsequently coiled onto a spool / hub. As part of a collaborative deployable space structures research effort between the National Aeronautics and Space Administration (NASA) and German Aerospace Center (DLR), a boom deployment system for a future 500 m² solar sail has been developed. To achieve the respective solar sail size goal, 16.5-m-long booms produced by NASA were integrated into a DLR-designed deployer mechanism. This considerable size, as well as the lightweight construction of the booms and respective deployable systems makes testing on the ground a significant challenge. Some systems for gravity compensation as well as vertical testing to minimize the influence of gravity have been used in the past. However, an uncertainty factor remains towards the behaviour in the space environment. The focus of this paper is the load application testing of the integrated boom-deployment mechanism system under microgravity condition, as well as a comparison to vertical testing under gravity. Testing in microgravity was performed during a parabolic flight test inside an aircraft and it included stowage and full deployment of a single boom along the longitudinal axis of the aircraft. The load application was split into two categories: static testing, which induced a linear force ramp to the static boom for either compression or compression-bending; and dynamic testing, which applied a constant force to a boom during extension provided by the deployer mechanism. Both types of tests were performed multiple times at two distinct lengths of the boom, fully deployed (12.76 m) and ~28.6 % deployed (3.65 m). More parameters that are vital to the test philosophy are the angles of attack in the force application and the highest force applied. The data acquisition used for the applied load and deflection measurements of the boom is also presented.

[1] Principal Investigator of the Microgravity Boom Experiment. Research Aerospace Engineer, DLR Institute of Lightweight Systems (formerly Institute of Composite Structures and Adaptive Systems).
[2] Principal Investigator of the Deployable Composite Booms project. Research Aerospace Engineer, Structural Dynamics Branch, AIAA Senior Member.
[3] Research Aerospace Engineer, DLR Institute of Lightweight Systems (formerly Institute of Composite Structures and Adaptive Systems), AIAA Member.
[4] Research Aerospace Engineer, DLR Institute of Lightweight Systems (formerly Institute of Composite Structures and Adaptive Systems), AIAA Member.
[5] Research Aerospace Engineer, Structural Dynamics Branch, AIAA Member.
[6] Research Aerospace Engineer, Structural Dynamics Branch, AIAA Member.

I. Introduction

Most high-technology-readiness deployable space structures are designed for medium-to-large-sized satellite and spacecraft applications. The lack of reliable deployable structural systems for low cost, small volume, rideshare class spacecraft, such as CubeSats, currently limits the potential of small satellite platforms for use in low cost science and exploration missions. Deep space missions where relatively large deployed structures are required for power, communications, and in some instances propulsion, are particularly limited. The National Aeronautics and Space Administration (NASA) is currently investing in the development of a new class of advanced deployable thin-shell composite booms to support future deep-space small satellite missions [1-3]. These boom concepts are being designed to meet the unique requirements of small satellites. These requirements include: packageable into very small volumes, testable on the ground in an Earth-gravity environment, inexpensive to manufacture, scalable for use as elements of hierarchical structures (e.g. trusses), capable of being stored for long periods without significant distortions in deployed shape, high deployment reliability, controlled deployment behavior, and predictable deployed dynamics.

The Deployable Composite Booms (DCB) project by NASA and the Joint Deployable Space Structures (JDSS) project by the German Aerospace Center (DLR) are collaborating to improve the state-of-the-art in rollable high strain composite booms and associated deployment mechanisms. The collaborative effort has the near term goal of perfecting booms for large CubeSat-class solar sails and other small satellite applications requiring 5-to-20-meter booms [4], and the medium term goal of producing much longer booms as well as boom trusses. NASA has produced 16.5-m-long rollable Collapsible Tubular Mast (CTM) booms out of high strain composite materials and tested with DLR the as-manufactured performance of these ultralightweight deployables in the laboratory, with and without flight-like boundary conditions [5].

The focus of this paper is the experiment methods and preliminary results of a microgravity test campaign performed in July 2021 to characterize the structural and functional behavior of a long deployable boom in a representative environment, as well as a comparison with vertical testing performed under gravity. In Section II, the details of the general setup of the microgravity test, such as the relative position of the deployment mechanism to the force application units and photogrammetry cameras arrangement, the test matrix and sequence are described. In addition, a comparison between the test setup for the microgravity and ground vertical tests and the stowage process of the boom during flight is presented. In Section III, the hardware components produced for the microgravity experiment, including the load application units and the photogrammetry cameras are described. In Section IV, the software developed to gather boom deflection and strain measurements with the photogrammetry cameras and the load data acquisition system are presented. In Section V, the experimental results of the microgravity and ground vertical tests are presented, and there is a comparison of the behavior of the boom under both environments that provides feedback to the two distinct test approaches. Conclusions from the test campaigns are presented in Section VI.

II. Experiment Description

The booms and deployment mechanism are designed for a square solar sail of 500 m² area, where the four diagonal booms each measure 16.5 m in length. Functional ground testing in the intended configuration of the solar sail, i.e. four booms arranged in a cross, has already proven to be challenging due to its size [6]. Such configuration at full scale is not possible inside a microgravity parabolic flight aircraft. Instead, a single boom from the cross was deployed and tested and loads were applied to emulate the forces required to tension the square solar sail. The test article used in the microgravity test campaign is shown in Fig. 1.

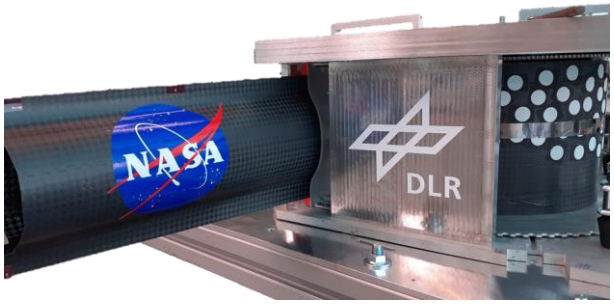

Fig. 1. NASA boom coiled inside the DLR deployer on the test rack in preparation for the parabolic flight test campaign.

A. General Setup

The experiment was arranged inside the Airbus A310[7] Zero-G aircraft operated by Novespace. A top and isometric view of the test setup in shown in Fig. 2. The majority of the test setup was mounted along the starboard side of the aircraft. The boom deployment mechanism was mounted towards the rear of the aircraft and the boom was deployed in the flight direction. The naming convention used was to consider the left side of the boom to face the starboard side of the aircraft and right side of the boom the port side. A number of elements are presented in Fig. 2, where the starboard side is the top of the image and the port side is the bottom. Position 1 denotes the boom deployment mechanism. Position

[7] Any mention of a product, vendor or analysis is for clarity and not an endorsement by the authors.

2 refers to the pairs of Force Application Units (FAU) located for testing at two different boom lengths. Position 3 refers to the seven sets of pairs of cameras used for photogrammetry. There is another set of photogrammetry cameras located on the boom deployment mechanism tracking the root of the boom. The dashed lines illustrate the field of view for one pair of these cameras (Handrail camera #1). Position 4 illustrates the location of the camera controller and computer.

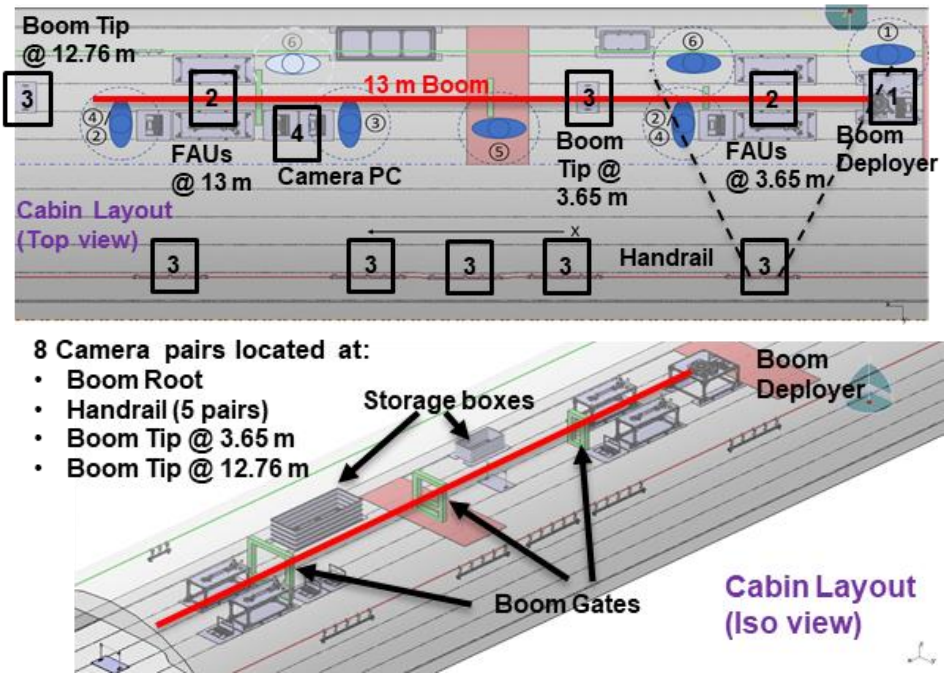

Fig. 2. Test setup: (top) aerial view, and (bottom) isometric view.

B. Emulation of Sail Forces

Simulations have shown that an effective way to tension the four sail quadrants of a square solar sail is to minimize moments on the slender booms and load them in such a way that the resultant force applied to each boom tip has an angle of attack (angle between the boom longitudinal axis and the load) smaller than 10° [7, 8]. Due to the volume limitation in the aircraft and other experiment stands, no sails were attached to the boom, but rather the forces were applied via strings under the desired angle of attack.

In addition to the ideal symmetric force application, where the angle of attack equals zero that results in compression-only loading of the boom, asymmetric tests leading to a combined compression-bending of the boom were performed. For both symmetric and asymmetric tests, an angle of attack of 10° was applied to the boom tip to cover a worst-case loading scenario.

C. Sequence of Tests

The parabolic flight test campaign consisted of thirty parabolas where the boom was subjected to different test conditions. The thirty parabolas were divided into six sets of five parabolas each. The time between parabolas within each set, when the plane recovered nominal cruise flight 1-g conditions, were about 60-s to 90-s long. In this paper 1-g refers to the average gravitational pull of the Earth of 9.81 m/s^2. This short time only allowed for minor reconfiguration of the test setup. However, between each parabola set, the 1-g phase was about 5 min long, and thus this time was used to change the test setup. A simplified sequence of the test matrix performed is given in Table 1.

Table 1. Tests performed per set of parabolas.

Parabola number	Group of tests
1-5	Static testing at 3.65 m
6-10	Dynamic testing at 3.65 m
11-15	Continuous boom deployment
16-20	Static testing at 12.76 m
21-25	Static testing at 12.76 m
26-30	Dynamic testing at 12.76 m

Each set of five parabolas was split into two symmetric and three asymmetric loading tests to obtain repeated results for pure compression and combined compression-bending loading from the left and right side of the boom. Ideally, the number of tests performed for a given boom length and load case could have been repeated more often, but a compromise given the limited number of test parabolas had to be made.

Boom load testing at the two distinct lengths was a consequence of previous ground tests performed at those lengths,

as well as related simulations performed [8]. The decision to perform a deployment test during one set of five parabolas was made for two reasons. It allowed for unique inspection of the deployment process during microgravity and reduced the time of breaks between sets of parabolas as the same boom specimen had to be extended from the initial 3.65-m-deployed length configuration to the final 12.76 m during the flight. More physical interaction between the boom and its deployment mechanism by deploying it in microgravity conditions, as well as the boom behaviour under this dynamic excitation could be observed during these parabolas. Although no external load was applied to the boom during this continuous deployment phase, it represented well an in-space operation of the boom and boom deployer system.

In general, the quality of the microgravity environment produced by the aircraft parabolic maneuver was very good. Each parabola provided about a 20-s-long microgravity phase with < ±0.03 g acceleration in all axes. Before and after the microgravity phase, the aircraft manuevering gradually induced 35-s-long hypergravity phases of ~1.8 g acceleration that transitioned rapidly to microgravity conditions at the apex of the parabolic trajectory. As an example, the accelerometer data from the aircraft for one of the parabolas (#2) is presented in Fig. 3.

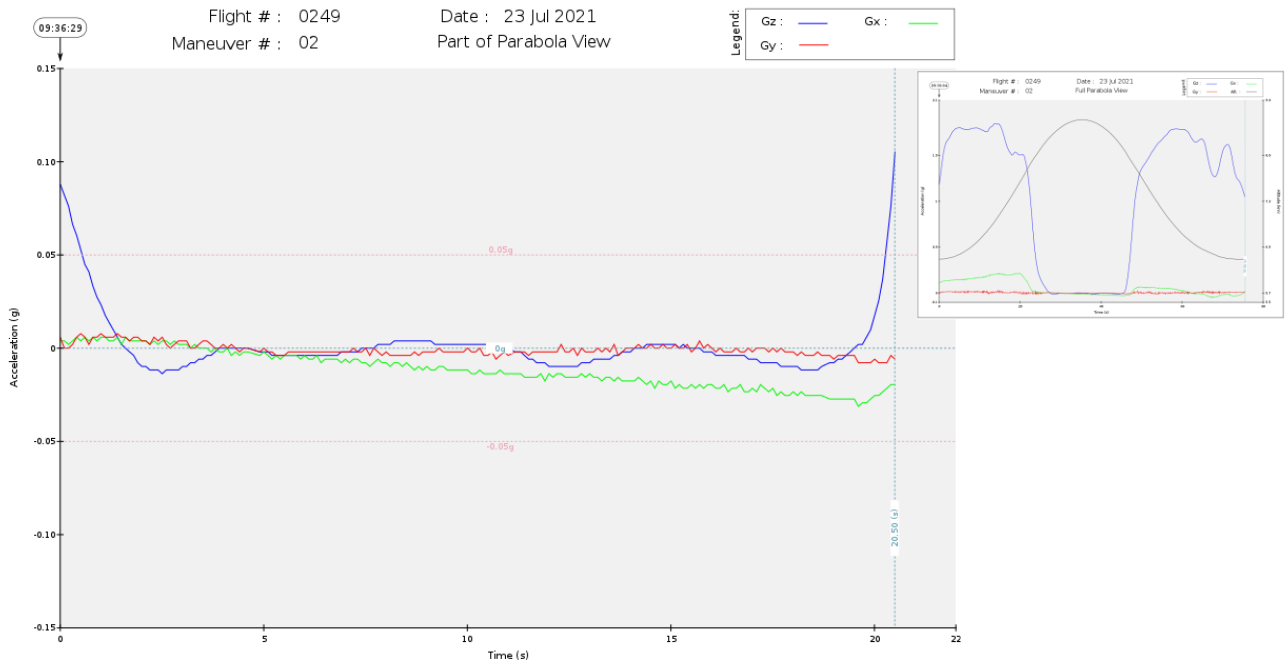

Fig. 3. Aircraft accelerations during the 20 s microgravity phase for Parabola 2: vertical z-axis (blue), lateral y-axis (red), axial x-axis (green). The inlet on the top right corner shows the accelerations for the entire 90 s parabolic maneuver.

D. Microgravity Test Comparison to Vertical Test Stand on the Ground

The test setup inside the microgravity aircraft needed to be comparable to a vertical test setup in a DLR facility used for previous 1-g ground tests on similar boom specimens. The 13.5 m tall test stand for 1-g vertical testing at DLR Braunschweig is shown in Fig. 4. The boom is hung vertically downwards from the boom deployment mechanism, which can travel on a cart up and down the test stand to setup the test height according to the boom length. Testing in a vertical configuration minimizes the effect of gravity on the thin shell slender structures and allows testing of different boom lengths. Booms from various projects have been tested and characterized in this manner prior to this effort [9-11]. The boom is loaded by the test frame in the basement. This frame loads the boom tip by pulling on a string that runs over a pulley system to a load cell. The position of the pulley can be adjusted to different load angles of attack. While simultaneously measuring force applied, a motion tracking videogrammetry system also tracks a number of reflective points on the boom tip to measure the resulting boom tip displacement.

The test setup inside the microgravity aircraft is shown in Fig. 5. This setup resembles the vertical test stand at the DLR facility but was arranged in a horizontal configuration to benefit from the long axis of the aircraft. The force application is applied by mechanical units at the left and right side of the boom that are positioned in the equivalent plane where the boom tip would connect to the adjacent solar sail quadrants. Rather than moving the deployment mechanism to desired distances from a single fixed force application unit to accommodate different boom length specimen as in the vertical stand, for the aircraft setup the entire load application hardware was doubled and pre-positioned according to the two predefined boom lengths to be tested. The force was applied at a 3.65 m and 12.76 m free lengths of the boom. The free length is defined as the length of unsupported boom, i.e., the distance between the boom exiting the guide shell inside the deployment mechanism and the tip of the boom.

Due to safety-related reasons, the aircraft tests were performed with smaller applied forces to avoid damaging the boom. The surrounding test frame was also reduced in size according to the smaller deflections imposed on the boom. Several foam gates were fabricated and placed along the boom path to contain the boom in case of an unexpected event during the parabolic flights.

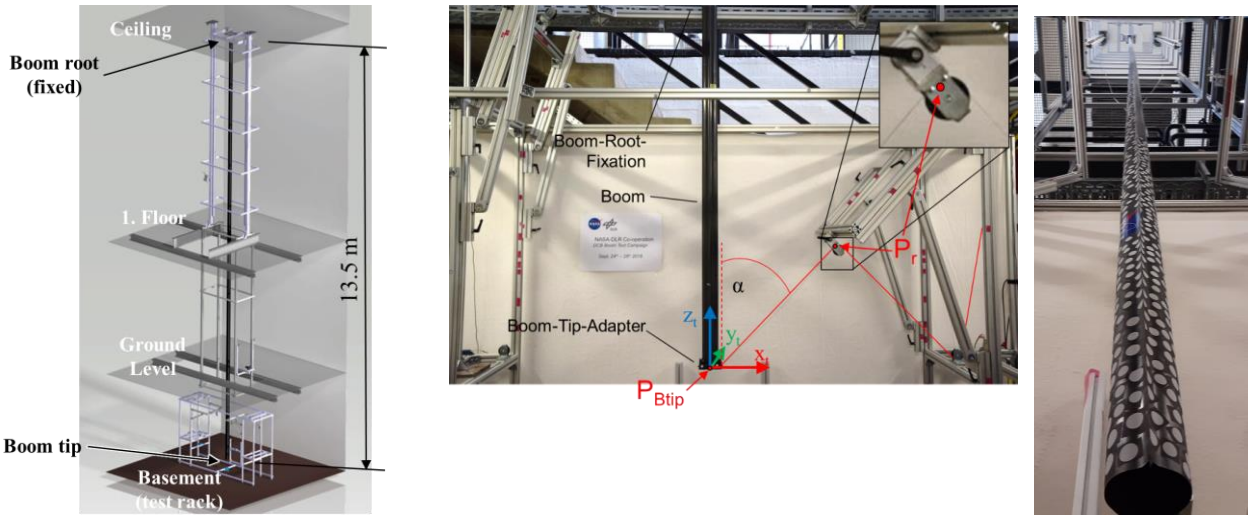

Fig. 4. Vertical test setup at the DLR facility with the boom hanging downwards.

Fig. 5. Preflight testing of all test procedures inside the aircraft for in-flight operations. Image shows the deployer mechanism with the deployed boom passing through the center of the three rectangular safety gates.

E. Stowage for Take-Off and Landing

One challenge arising from the load angle of attack being 10° and the limited space within the aircraft was the angular shift of boom exit direction during deployment, which is related to the decreasing diameter of the coiled boom on the spool [12]. In the vertical test stand, different adapter plates based on the boom length to be tested were fabricated to align the boom axis with the direction of gravity defined by a vertical plummet. In the aircraft setup, the entire deployment mechanism was rotated twice during operation with respect to the fixed test rack to account for this angle shift to keep the boom path relatively straight for all parabola setups.

Contrary to ground deployment where the boom can rotate over the floor, the setup within the aircraft needed to be aligned with the aircraft's long axis, parallel to the flight direction. This setup resulted in the deployment mechanism needing to be turned on its test rack. The turntable used during ground testing did not fulfill the safety requirements, so a pin-and-clamp solution with two distinct positions was established. This approach allowed the deployment mechanism with the stowed boom inside it to be removed from the test rack during the aircraft take-off and landing phases while allowing it to be secured in the correct orientation during flight. Positioning drop-in pins were used to guarantee the correct angle of the mechanism, before fixing it in place with clamps that were designed to hold the deployment mechanism in case of any loads other than gravity (Fig. 6). The single rotation was performed during the break between

parabolas 15 and 16, with 8 m of boom already deployed before continuing to deploy to the full length. The need to remove the deployment mechanism from the test rack for landing also required complete boom coiling after the final parabola, which added 30 minutes to the total test time required in 1-g cruise flight.

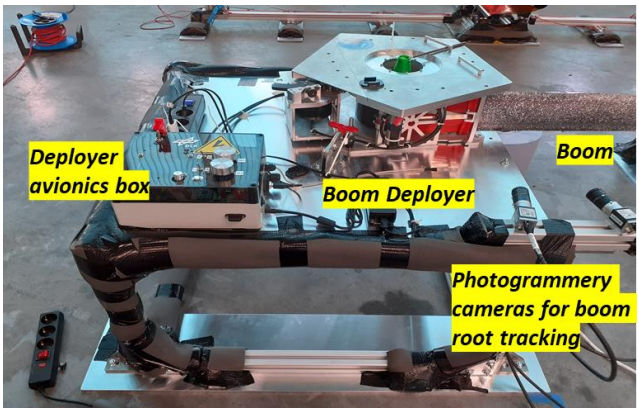

Fig. 6. Deployment mechanism clamped down on its test rack.

III. Microgravity Experiment Components

The deployment mechanism has been designed for the joint research effort between NASA and DLR [12, 13] to support this specific type of boom [5-8]. However, within the scope of the international cooperation, two components have been produced specifically for the parabolic flight test campaign.

A. Force Application Units

To enable symmetric boom load testing and asymmetric loading from the left and right sides for the two different boom lengths/positions, the test setup features a total of four identical force application units (FAU) arranged in two pairs. The DLR Braunschweig team developed the FAU. Each unit is primarily equipped with a linear drive component and a force sensor. The drive unit applies a linear displacement that is transferred to the boom tip by a string and pulley. During this action the resulting force is measured by a load cell in line with the string. For safety reasons and to limit the motion of the boom, the load application is halted at 5 N and reverted quickly afterwards to release the tension in the string.

A pair of FAU arranged at either side of the deployed boom is shown in Fig. 7. Besides the necessary driving electronics of the FAU and the test rack structure, the red strings that connect to the boom tip for loading and the linear drive train with the motor can be seen. The two FAU in one position work together symmetrically to create a compression load on the boom as illustrated in Fig. 8 (a). By releasing either of the strings, an asymmetric load could be applied, resulting in a compression-bending of the boom. The dashed lines indicate the field of view for a pair of cameras looking at the boom tip.

For the static tests carried out during parabolas #1-5 and #16-25, the boom was positioned in place with the strings slacked. The motorized drive train translates the cart where the root end of the string is fixed, applying load at the boom tip end. The rate of motion of the cart was 1 cm/s during the quasistatic load application phase. Upon reaching 5 N of tension in the string, the cart was driven quickly to the initial position to unload the boom.

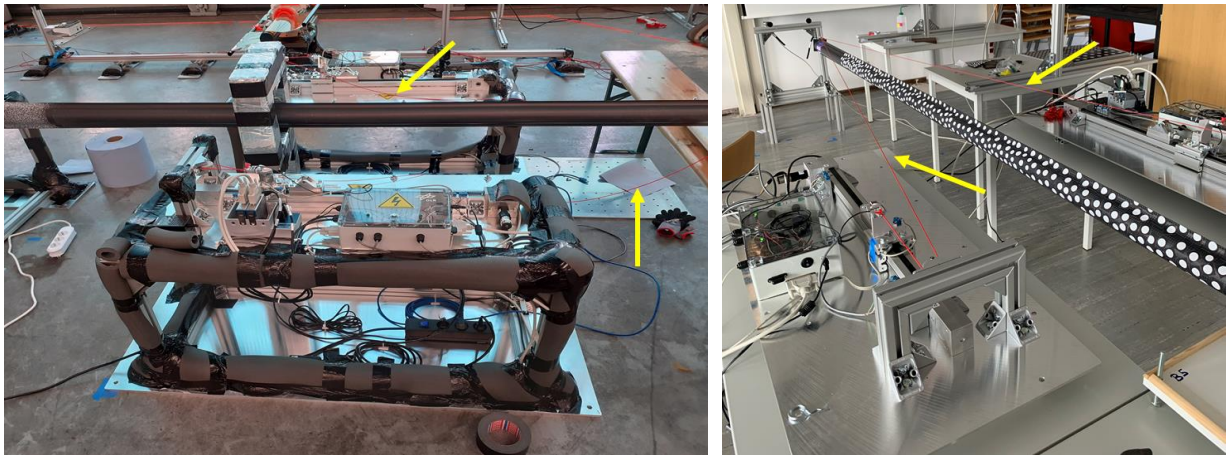

Fig. 7. Two parallel force application units with a boom in between during ground testing. Note the red-colored loading strings are slack on the left image and tensioned on the right image. Yellow arrows have been added in the images for clarity of locating the strings.

For the dynamic tests, each FAU was equipped with a 5 N constant force spring. The test procedure had the linear drive trains remain fixed in position while the deployment mechanism extended the boom for several seconds. This test replicated the more realistic dynamic load scenario of extending the booms while deploying the sail segments and finally tensioning them to a higher load. This type of test was not performed in the vertical test stand at DLR and was identified as the type of test ideal for being performed under a microgravity condition.

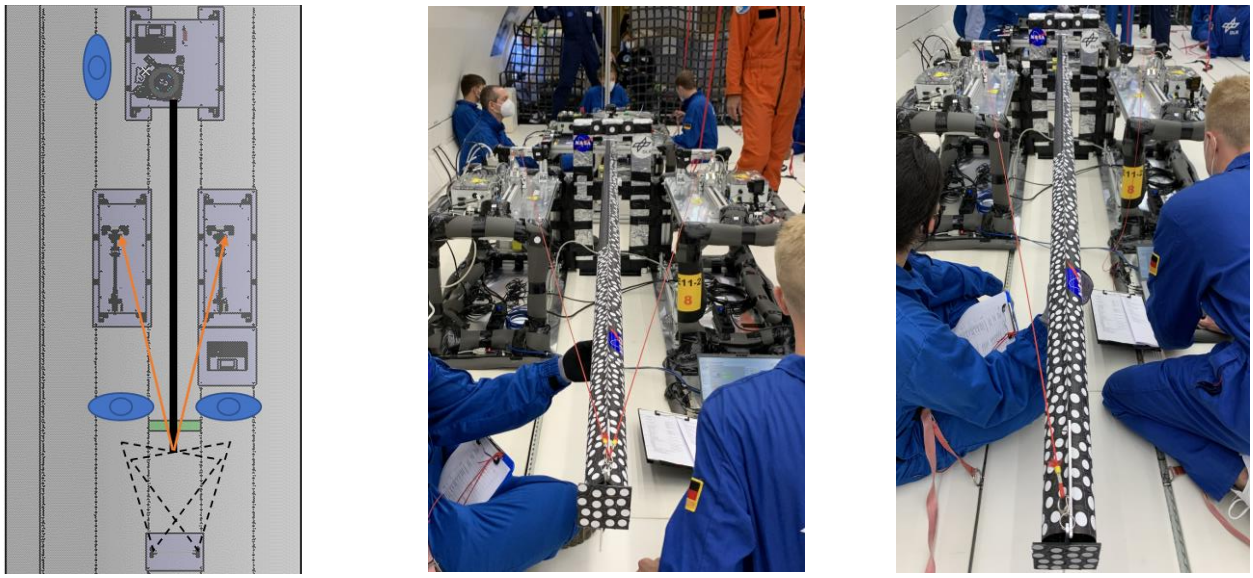

(a) (b) (c)

Fig. 8. (a) Drawing of the load application test setup at 3.65 boom length; and flight test configuration for: (b) symmetric testing, and (c) asymmetric left side test.

B. Photogrammetry Camera System

The team at NASA Langley Research Center developed a large-scale sixteen-camera photogrammetry system capable of tracking the deflections and strains of the boom while being loaded and/or deployed. Eight pairs of stereo optical cameras were used during the microgravity test campaign. Five sets were fixed to the aircraft handrail running along the long axis of the cabin on the port side to get complete coverage of the 13-m boom test article from a lateral view. The handrail cameras mounted on the aircraft during use in flight are shown in Fig. 9 (left). These cameras were used to get a global shape of the boom during the various tests. Another pair was placed in front of the boom tip about 1 m from it when the boom was deployed to the 3.65 m length. This camera pair looked edge onto the boom and tracked the boom tip deflections. After the first ten parabolas, this camera set was not used and the boom was deployed to a larger length by passing between the pair of cameras. This can be seen in Fig. 9 (right). A set of cameras fixed to the boom deployment mechanism test rack were positioned to get a side view of the boom root during all parabolas to capture the local deflections and strains in such a critical area. An additional camera set was located in front of the boom tip when this was deployed to the 12.76 m free length. This camera pair looked edge onto the boom and tracked the boom tip deflections during parabola #16-30. They can also be seen in the front area of Fig. 9 (left).

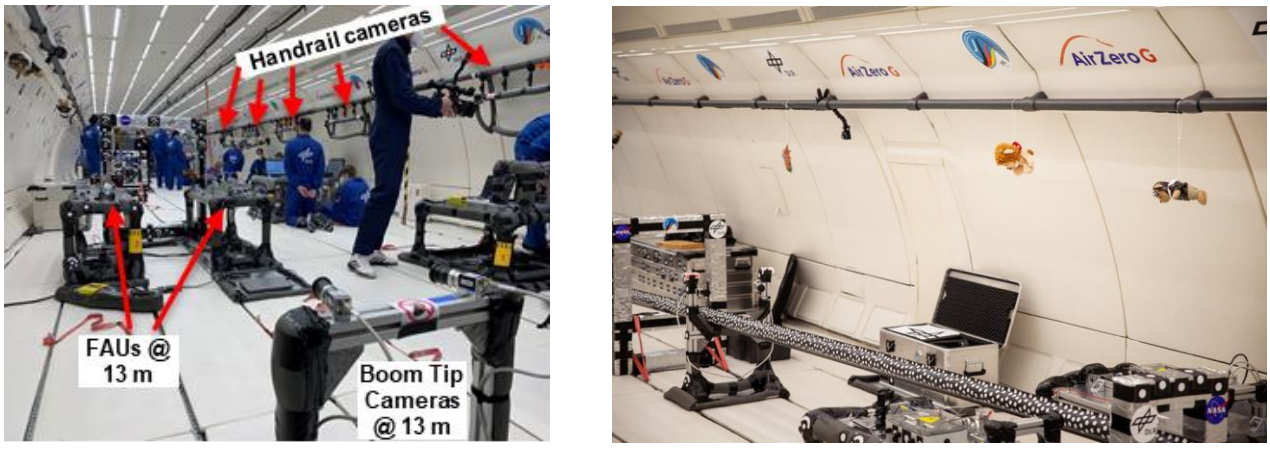

Fig. 9. (left) Full test setup installed in the aircraft cabin showing the location of the five pairs of handrail cameras and the FAU and boom tip cameras for the final full-scale tests; (right) boom deployed for calibration of the photogrammetry cameras the day before the flight showing the white dotted pattern on the carbon fiber boom used for motion tracking. The boom tip cameras that track the tip at the deployed boom length of 3.65 m is shown.

All camera sets were synchronized and controlled from a single computer and user on board with the use of custom-built software that took synchronized images at a specified rate of 4 frames per second (fps). To synchronize the boom displacement/strain data measured with the camera imagery to the load application data gathered by the FAU, the latter unit flashed a light at the beginning of the test that the cameras picked up. This event was used to zero both sets of test data during post-processing. The entire test area inside the aircraft with all test racks installed is shown in Fig. 10.

Fig. 10. Full test setup installed in the cabin after camera calibration.

C. Boom gates

In addition to the two necessary technical systems to perform the test, three boom gates of increasing size were placed along the deployment path of the boom. These gates were made out of soft foam and subsequently coated in aluminized-tape to comply with fire hazard safety regulations imposed by the aircraft operator company. By limiting the range of free motion of the boom, the gates prevented damage to the boom and prevented it from injuring operators or interacting with other flight experiments in the cabin. A look into the deployment direction through the aligned boom gates is shown in Fig. 11. The two sets of cameras used for tracking the displacements of the boom tip at each length tested can also be seen.

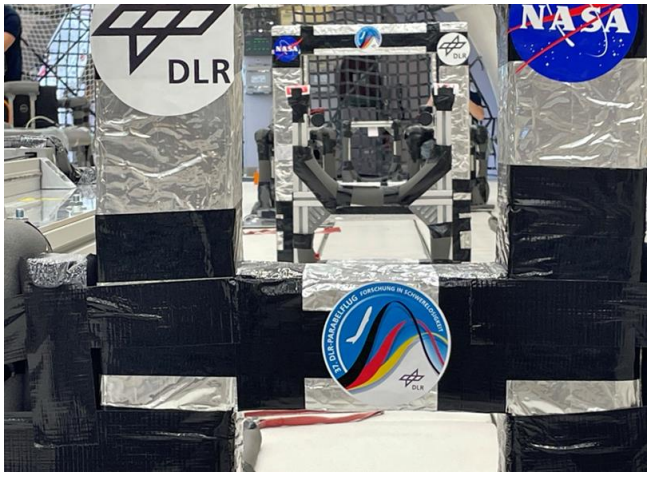

Fig. 11. Aligned boom gates.

IV. Microgravity Test Data Acquisition

A. Stereo photogrammetry

The goal of the photogrammetry system is to measure the global deflection of the boom, including that of the boom tip, for redundancy since that is a critical area for determining the behaviour of the boom under loading. In addition, the camera pair at the root of the boom was used to measure the local full-field strain of the first 30-cm-long section of the boom as it exited the guide shell inside the boom deployer. That area was identified as a potential location for local or global buckling under load.

The entire right side of the black-colored carbon fiber/epoxy boom was covered with 12-mm-diameter white targets. Also, targets were applied in the first 2 m section from the tip at the left side of the boom, as initially an additional set of cameras was going to be used to track that boom section for redundancy. The targets had an adhesive backing and were added manually to the boom in a random pattern. A lightweight 10 cm x 10 cm area plastic plate was bolted to the front face of the boom for the two sets of boom tip cameras to track. The white-dotted pattern along the boom and the flag at the boom tip can be seen in Fig. 8 (b) and (c). For the cameras tracking the local strains at the boom root, a white speckle random pattern with targets smaller than 1 mm was sprayed on the left side of the boom.

The ARAMIS 2020© software developed by GOM Metrology was used to process the stereo imagery from each camera set. A picture taken during Parabola 3 from the first camera set at the handrail is shown in Fig. 12. This test was a static asymmetric load case where the boom was loaded towards the right side. The field of view from this stereo camera set covered a boom span of about 3 m. The contour color plot shown in Fig. 12 indicates the lateral displacement (side-to-side direction) of the boom at a certain frame rate during the test. As expected, the red-colored area that corresponds to larger values of lateral deflection is towards the boom tip and the blue-colored region that corresponds to the smaller values of lateral deflection is towards the boom root in the section of the boom that was analyzed by the digital image correlation (DIC) software. The processed lateral displacement of the root section of the boom for the same test in presented in Fig. 13. In the view shown, the color scale corresponds to out-of-the-page deflection of the shell. It can be seen that a local buckle formed near the top section of the thin-shell boom indicated by a dimple with an abrupt change in deflection (red and blue color). This type of local buckle formed during the hypergravity phase (1.8 g) of the parabola that naturally occurs prior to the aircraft reaching microgravity conditions. The test operator manually held the boom tip during this hypergravity phase until microgravity was reached and then released the boom. At that moment, the local buckle disappeared. After a few seconds, the tip load was applied by the FAU and the real test began.

Fig. 12. Partial field of view measuring lateral side-to-side displacement of the boom with the photogrammetry system.

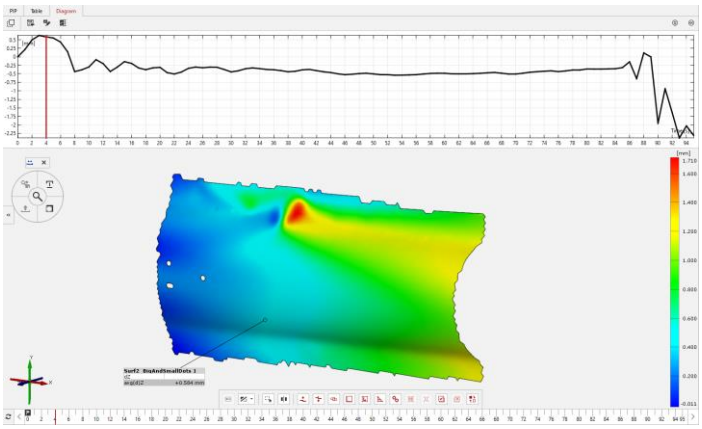

Fig. 13. Lateral side-to-side displacement of the boom root showing the buckle formation during the hypergravity phase of the parabolic flight.

B. LabView Recordings

The FAU used Labview to control and record the load data applied to the boom. Representative load test data from the left (blue) and right (orange) FAU are shown in Fig. 14. Both are from symmetric tests that used both FAU. The results from a static test are shown in Fig. 14 (a), where the 5 N maximum load was reached and then quickly released. The results from a dynamic test are shown in Fig. 14 (b), where the 5 N was reached via extension of the constant force springs and then held relatively constant while the boom deployed against the springs.

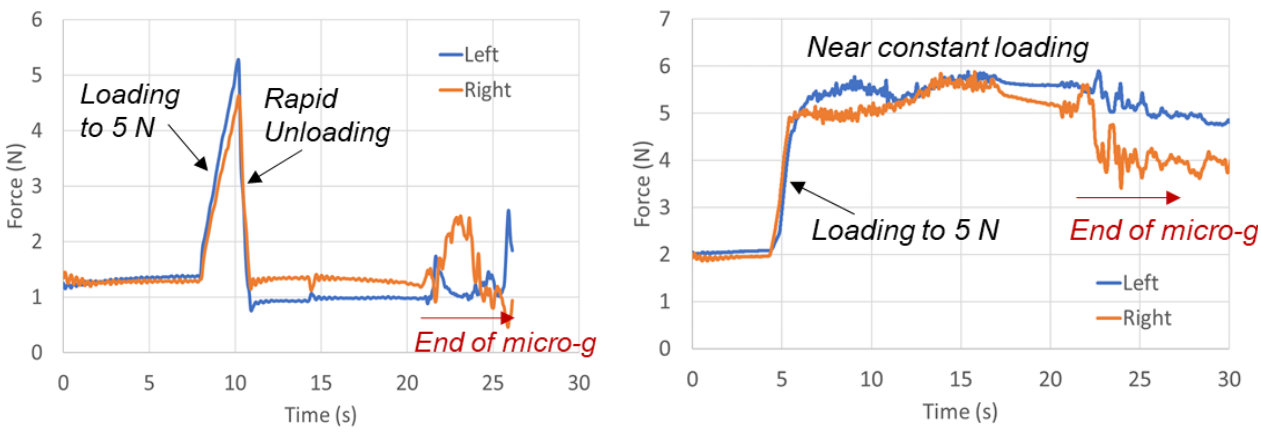

(a) (b)

Fig. 14. Force data taken during: (a) static symmetric test 1 (Parabola #1); (b) dynamic symmetric test 2 (Parabola #10).

V. Experimental Results

Partial results from the in-flight boom experiments for comparison with the post-flight quasi-static ground experiments carried out at the DLR's vertical test stand using the same boom test article are described in this section. Due to the ongoing analysis of the large amount of flight test data gathered from the photogrammetry system, further results are expected in a future dedicated publication. In this paper, the acquired boom test data, as described in Sections III and IV, are analysed for the 3.65-m and 12.76-m deployed lengths mainly for the asymmetric load cases.

A. 1-g ground experiments

For ground testing under a 1-g environment, the 3.65-m deployed boom length was tested in asymmetric and symmetric loading conditions. For the 12.76-m deployed boom length, although similar tests were carried out, the analysis so far is focused on the asymmetric loading condition. The post-flight mechanical test in the vertical test stand produced the results depicted in the load-displacement graphs of Fig. 15. These load-displacement curves were acquired in seven to eight subsequent test runs loading each side (left and right) of the boom. The response curves from the 3.65-m boom shows some non-linearities for both loading directions as illustrated in Fig. 15 (a). This non-linearity can be attributed to local buckling occurrences near the guide shell at the boom root. To provide comparable stiffness values for both boom length scales tested, an absolute lateral tip displacement (x-axis) range of 10 mm to 100 mm was used to determine the slope of the load-displacement graphs via linear regression, as depicted in Fig. 15 (c) and Fig. 15 (e).

This approach proved to be more necessary for the 12.76-m boom. The larger-scale test article presents a highly non-linear region in the load-displacement curve beyond the initial linear region at boom tip displacements under 100 mm, as shown in Fig. 15 (b). This response was already observed in previous experiments of a similar boom [8]. It is assumed to have its origin in the changing angle of attack when displacing the boom tip, as the compression component (acting vertically) increases due to the changing path of this part of the tip load that is contributed by boom tip mass and boom self-weight. Therefore, determining boom stiffness, c, using small tip displacements below 100 mm provides reasonable results, as validated by the good linear fit observed in Fig. 15 (d) and Fig. 15 (f) for the 12.76-m case.

B. Microgravity in-flight experiments

Similar to the 1-g tests, boom tip loading and displacements were analysed for the in-flight microgravity experiments. The load-displacement curves are provided in Fig. 16 and Fig. 17 for the 3.65-m and 12.76-m boom deployed length test configurations. The symmetric load case is presented in Fig. 16 (a), while asymmetric cases to the left and right are shown in Fig. 16 (b)-(c) and Fig. 16 (d)-(e). As boom stiffness was again determined by the slope of a near linear region of the load-displacement curve, the main difference compared to the 1-g experiments is the smaller range of displacements used for data generation. For the symmetric load case of the 3.65-m length (Fig 16 (a)), a range of lateral boom tip displacement of up to 5 mm was analysed, while for the asymmetric cases a range of displacement of up to 100 mm and 200 mm for the right and left side loading direction were analysed.

The load-displacement curves generated for Parabola 20 (12.76-m scale) are provided in Fig. 17. The lateral boom tip displacement data presented were gathered from two cameras sets, one in front of the boom tip, and the other from the handrail to the side of the boom tip, which tracked a section of the boom starting 1.5 m from the boom tip. Note that this data is generated from the start of a symmetric load test where the boom was pulled from the right string only and is therefore considered a pseudo right asymmetric case. Both response curves show some non-linearities, as the boom was greatly affected at larger scales by the dynamics of the aircraft and the manual operator's release prior to the start of the test. In fact, a large number of parabolas when the boom was fully deployed to 12.76 m rendered unusable displacement data during the loading step as the rapid motions of the boom were not captured adequately with the 4 Hz frame acquisition rate of the photogrammetry system. Such dynamic response was not observed during preparatory ground experiments of

the flight test campaign and it was exacerbated in asymmetric load cases as the boom tip was less restrained. A faster frame rate was not possible to implement due to the number of camera pairs used and data bandwidth constraints. When a higher frame rate was targeted during ground experiments, the chances of losing pictures from cameras was higher so a compromise on the frame rate was adopted to reduce the risk of missing critical data.

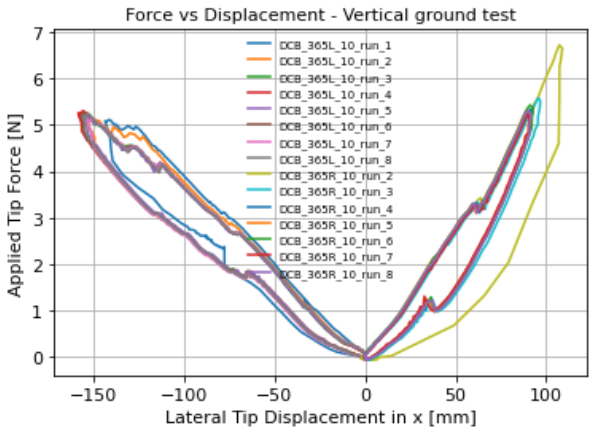

(a) 3.65 m – asymmetric

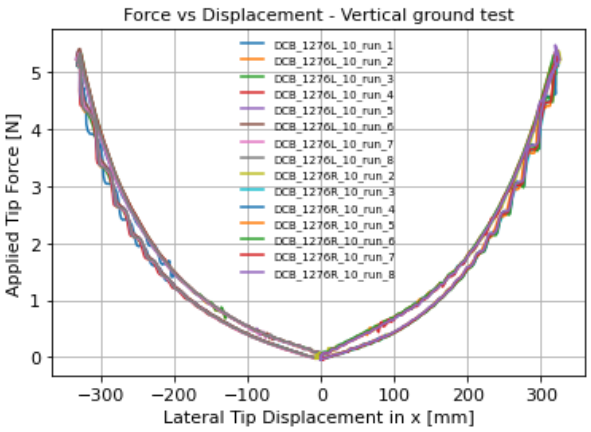

(b) 12.76 m – asymmetric

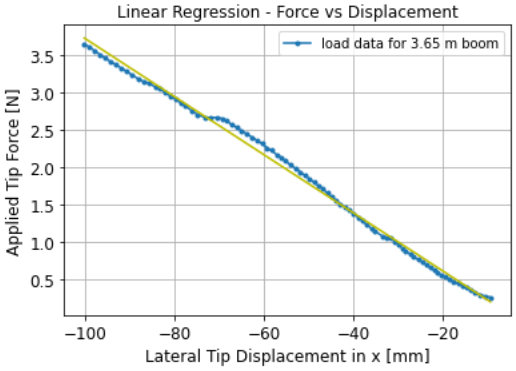

(c) 3.65 m – asymmetric left

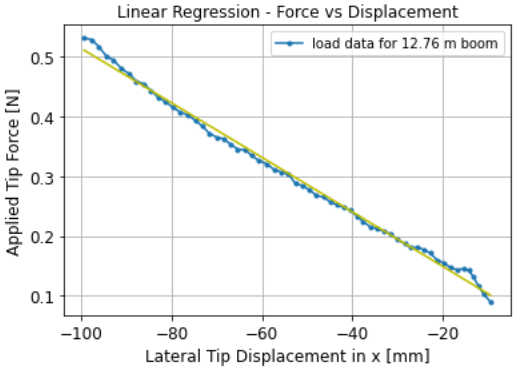

(d) 12.76 m – asymmetric left

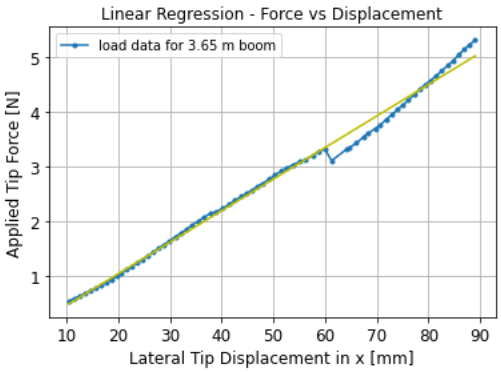

(e) 3.65 m – asymmetric right

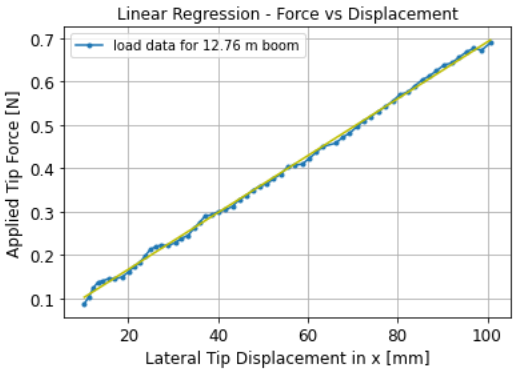

(f) 12.76 m – asymmetric right

Fig. 15. Load-displacement curves of the asymmetric compression-bending tests in a 1-g environment for the 3.65-m cases in (a), (c), (e) and 12.76-m cases in (b), (d), (f).

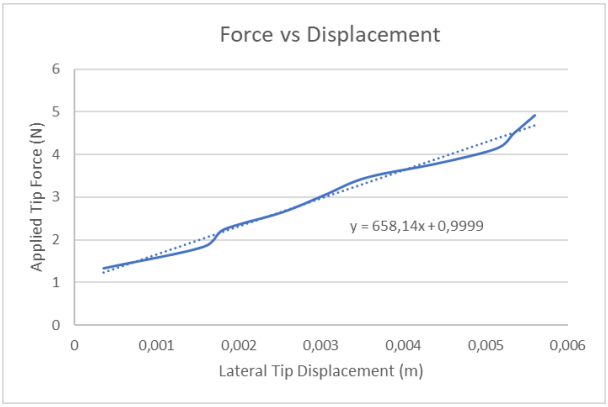

(a) Parabola #1 – 3.65 m – symmetric

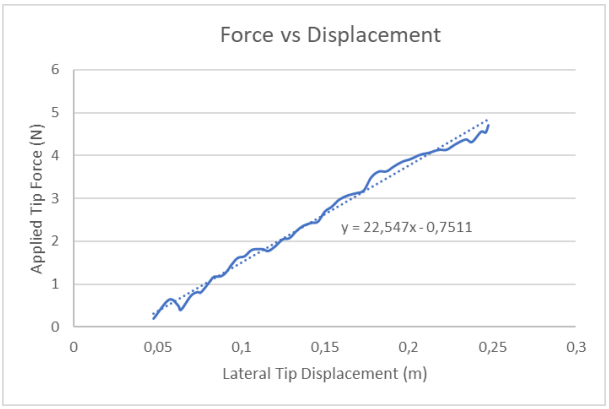

(b) Parabola #2 – 3.65 m – asymmetric left

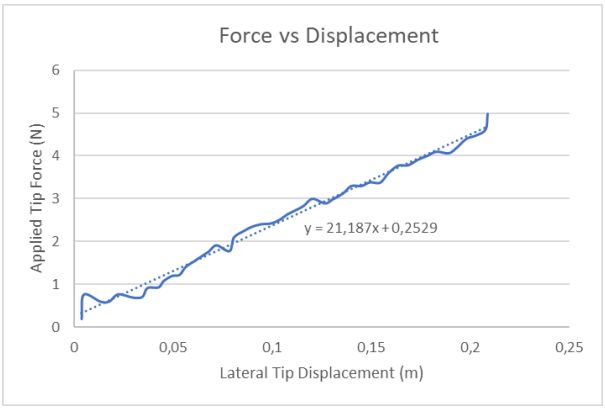

(c) Parabola #3 – 3.65 m – asymmetric left

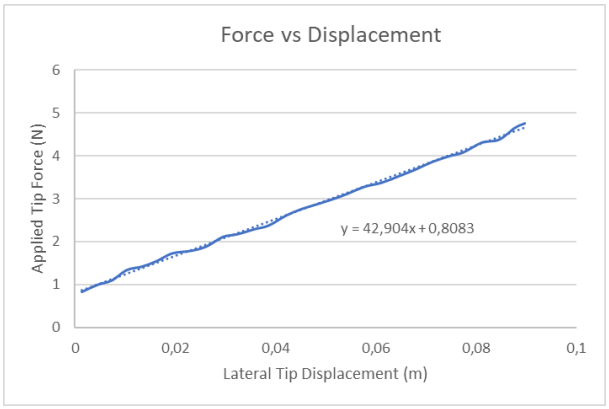

(d) Parabola #4 – 3.65 m – asymmetric right

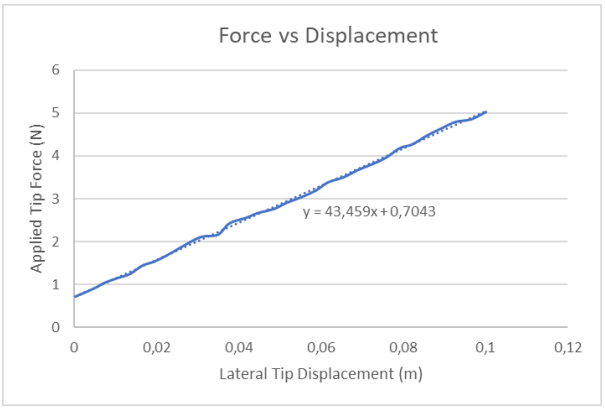

(e) Parabola #5 – 3.65 m – asymmetric right

Fig. 16. Load-displacement curves for the symmetric (a) and asymmetric (b) to (e) compression-bending tests of the 3.65-m deployed boom in a microgravity environment.

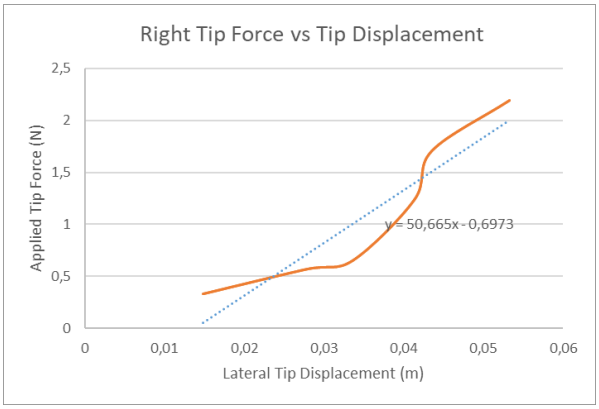

(a) Parabola #20 – displacement with front camera

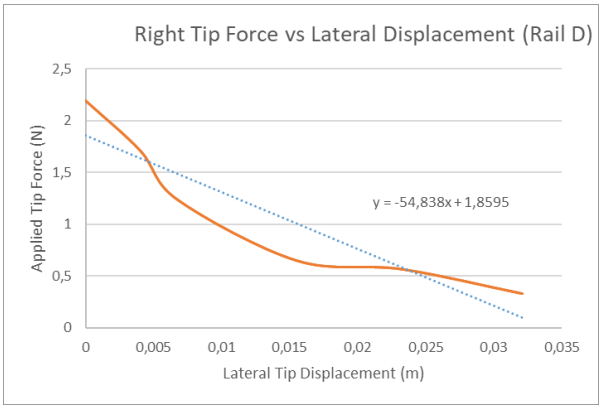

(b) Parabola #20 – displacement with side handrail camera

Fig. 17. Asymmetric compression-bending results for a 12.76-m deployed boom case in a microgravity environment. The boom tip displacement data was captured from: (a) boom tip cameras, and (b) side handrail cameras.

C. Comparison of Results

For comparison of each test configuration run in the microgravity and 1-g experiments, the results are given in terms of the slope of the load-displacement curves, k, also referred to as elastic stiffness, and the beam bending stiffness, EI. The results comparison for the 3.65-m boom length are presented in Table 2. Note that the bending stiffness EI is a length-dependent variable determined using the elastic stiffness k and the unsupported boom length l with 3.65 m for the short and 12.76 m for the long length test configuration. This relationship is found in Eq. 1 and follows the cantilever beam equation with a lateral tip load, and thus is a simplification of the test conditions since the axial load component is neglected, as are the gravity-induced loads for the 1-g vertical test. However, it is used here for a simple direct comparison of the results from different test configurations.

$$EI = k \cdot l^3/3 \tag{1}$$

At this point, most of the processed data is available for the 3.65-m deployed length cases. The results of the asymmetric cases in microgravity as given in Table 2 can be considered repeatable for each loading direction. As seen from the slope, k, and bending stiffness, EI, values, there is a significant difference in boom stiffness at the 3.65-m scale between asymmetric cases from the left and right side in both 1-g and microgravity conditions. The stiffness values for the left cases in microgravity are about 50 % lower than stiffness when loaded from the right side. As shown in Table 3, similar boom stiffness asymmetry can be observed for the 1-g vertical test results with 32% lower stiffness values for left-side loading at a 3.65-m deployed length, and 30% lower stiffness values for left-side loading at a 12.76-m scale, compared to the right cases. This difference can be traced back to the asymmetric fixation at the root of the boom due to the guide shell design. Therefore, it can be concluded that the right side of the system is stiffer than the left side, independent of gravitational influences.

When comparing elastic stiffness, k, and beam bending stiffness, EI, of each side between 1-g and microgravity tests at the 3.65-m scale, ground-based results show higher values of about 44% for left-side and 25% for right-side loading. The differences observed between microgravity and 1-g experiments at the 3.65-m scale are statistically significant. As mentioned previously, the higher stiffnesses measured in vertical ground experiments are considered to have the origin in the artificial stiffening effect from the mass of the boom itself and the boom tip interface that relieves some of the applied compressive tip load. Correlation of finite element boom models that included gravity to similar 1-g vertical tests were already presented in a previous paper and identified the gravity-induced stiffening phenomenon and the effects on the boom behavior [8]. The apparent discrepancy of results by an order of magnitude of the 1-g tests compared to the microgravity tests for the 12.76-m cases, as provided in Table 3, are not conclusive at this point and need to be revisited with more processed flight data and further finite element model correlation.

When comparing 3.65-m cases versus the 12.76-m cases in microgravity conditions, both scales present linear responses. The elastic stiffness, k, values for right side asymmetric loading are similar with 50.67 N/m and ~ 43 N/m, respectively. It is expected that this 20% discrepancy will reduce when further cases get post-processed as this was one of the reasons to perform this type of testing at two scales. This result makes the further point that scalability testing and analysis, as would be needed for even larger versions of the booms, is best addressed under 0-g or microgravity conditions that remove orientation and scale dependence response due to gravity. There is an order of magnitude discrepancy between the vertical 1-g test results when comparing k for the 3.65-m and 12.76-m cases. For the shorter scale, the boom self-weight and tip mass is assumed to be smaller than the compression component of the tip load putting the vertical boom in a true compression-bending state. However, for the long boom at 12.76 m, the hanging boom is in a tension-bending state and the root is relieved from some of the compression load as the test progresses. The boom root moment response is also known to be softer under compression and this produces a highly nonlinear response, as seen in Fig. 15 (b), that is path dependent in the load-displacement curve [8]. This boom-scale-dependent coupled effect in vertical 1-g testing could be investigated in the future by: gravity off-loading testing, for example with balloons in horizontal testing, by testing with asymmetric two-sided compression in the same vertical test stand, by testing vertically with the boom fixed at the bottom and loaded at the top to invert gravity effects, or by intensive shell-element finite element analysis.

The symmetric loading response of the boom at a 3.65-m length scale in 1-g vertical experiments is about 65% higher than in microgravity condition (k is 1087.54 N/m vs 658.14 N/m). The higher elastic stiffness values measured in the 1-g experiments can be explained by the stiffening effect of the mass of the boom itself and the boom tip fixture. Moreover, there is also the question of the as-manufactured boom shape not being perfectly straight and thus providing an “unknown” asymmetric load condition with tensioning from both sides, rather than the pure-compression symmetric case that is intended. In addition, the measured in-flight data were influenced to some extent by movements during hypergravity and microgravity phases induced by the airplane maneuvering, the varying residual microgravity, and the test operators manual release of the boom at the start of the microgravity phase. Nevertheless, the symmetric cases are more prone to errors because the displacements involved are so small that errors in them greatly affect the stiffness value in return.

Table 2. Test results for the 3.65-m boom length.

Test type	*Parabola*	*Load type*	*Slope/ Elastic Stiffness k [N/m]*	*Bending Stiffness EI [N/m^2]*
microgravity	#1	symmetric	658.14	-
microgravity	#2	asymmetric left	22.55	365.52
microgravity	#3	asymmetric left	21.19	343.47
microgravity	#4	asymmetric right	42.90	695.37
microgravity	#5	asymmetric right	43.46	704.45
vertical test stand (ground)	-	symmetric	1087.54	-
vertical test stand (ground)	-	asymmetric left	39.00	632.22
vertical test stand (ground)	-	asymmetric right	57.80	936.95

Table 3. Test results for the 12.76-m boom length.

Test type	*Parabola*	*Load type*	*Slope/ Elastic Stiffness k [N/m]*	*Bending Stiffness EI [N/m^2]*
microgravity	#20	asymmetric right	50.67 – 54.84	-
vertical test stand (ground)	-	asymmetric left	4.65	3216.86
vertical test stand (ground)	-	asymmetric right	6.59	4565.92

VI. Concluding Remarks and Outlook

In the collaborative framework of the Joint Deployable Space Structures (JDSS) project by DLR and the DCB project by NASA, the boom characterization data are shared between both partners and evaluated. It has been presented how ground and flight support equipment was used to gather valuable data to characterize the structural response of a slender thin-shell composite structure. Moreover, the differences in boom response between tests in microgravity and vertical 1-g conditions was presented, highlighting the deficiencies and challenges of each type of test configuration.

While the microgravity tests provided a seemingly easier scalability analysis of the test data as the beam stiffness at both scales is similar, it also proved more challenging to get a more controlled and stable test environment, as the parabolic aircraft dynamic conditions and manual operator errors were exacerbated at larger scales. If another parabolic flight test campaign is carried out, an automatic release of the supported boom at the start of the microgravity phase should be implemented to reduce the likelihood of dynamics induced in the test specimen by manual operator error. A better stiffness correlation between similar microgravity cases tested at different deployed boom lengths is expected when more processed flight data is available, as this was one of the reasons to perform this type of test at two scales.

The vertical ground testing, while being more repeatable and controllable at every test scale, provided an additional loading factor (gravity) that was found to affect and complicate results, particularly at the larger scale, and thus requires computational correlation for truly characterizing the response of the boom in the intended space environment. The highly nonlinear tip-load-displacement curves observed in all 12.76-m boom cases tested in 1-g conditions are in disagreement with the linear response measured in microgravity or at the shorter 3.65-m scale. It is recommended that in the future, more gravity off-loaded tests are carried out on long specimens, or the booms are ground tested by hanging them upwards and downwards to remove gravity effects. A modal survey test of the deployed boom is the next logical step to further refine the computational models being developed.

Significant loading directional dependence was measured in the boom stiffness regardless of the length-scale tested or the test method used due to the asymmetry in the boundary condition at the root of the boom provided by the deployment mechanism. This dependence is likely not a desirable feature for a component of a solar sail system that is arranged symmetrically (four booms in a cross that are equally loaded). Therefore, further refinement of the boom root boundary condition would be beneficial to the boom-deployer to maximize the loading capability of the entire system, as have already been implemented in other boom systems.

Acknowledgments

This research has been carried out under an Implementing Arrangement between NASA and DLR for Cooperative Research on Deployable Composite Booms. The research took place in the framework of the JDSS project of DLR and DCB project of NASA, where the data are shared between both partners and evaluated. The authors would like to thank DLR´s Space Research and Technology directorate and its former chair Prof. Dr. Hans-Jörg Dittus, the DLR institute director Professor Martin Wiedemann, as well as the head of DLR Department of Composite Design Prof. Dr. Christian Hühne for funding and supporting the microgravity test campaign. Moreover, the authors would like to acknowledge the work of others from the NASA DCB project team.

References

[1] Fernandez, J. M., "Advanced Deployable Shell-based Composite Booms for Small Satellite Applications Including Solar Sails," in *4th International Symposium of Solar Sailing*, Kyoto, 2017.

[2] Fernandez, J. M., “An Advanced Composites-based Solar Sail System for Interplanetary Small Satellite Missions,” in *AIAA Scitech*, Kissimmee, Florida, 2018.

[3] Wilkie, W. K., Fernandez, J. M., Horner, S., Brown, P. L., Banicevic, P., Denkins, T., Stohlman, O. R., Rose, G., Warren, J. E., Schneider, N., Dean, G., Kang, J. H., Chamberlain, M. K., Straubel M., and Heiligers, J.,"An Overview of NASA's Advanced Composite Solar Sail System (ACS3) Low Earth Orbit Technology Demonstration Project," in *AIAA Scitech*, Virtual Event, 2021.

[4] NASA Space Technology Mission Directorate, "Deployable Composite Booms (DCB)," https://www.nasa.gov/directorates/spacetech/game_changing_development/projects/dcb/ [Accessed 23 November 2022].

[5] Fernandez, J. M., Krizan, S. A., and Dyke, E. R., "Thin-shell Composite Booms for Solar Sails: Design, Manufacturing, and Qualification," in *5th International Symposium on Solar Sails*, Aachen, Germany, 2019.

[6] Richter, M., Straubel, M., Müller, D., and J. M. Fernandez, “Full Scale Flat Floor Testing of a 500-2²-Class Solar Sail Deployer,” in *17th ECSSMET*, Virtual Event, 2021.

[7] Stohlman, O. R., Chamberlain, M. K., Fernandez, J. M., Zander, M. E., and Wilkie, W. K., "Structural Modeling of a Composite-boom-deployed Solar Sail with Realistic Part Variability," in *5th International Symposium on Solar Sailing*, Aachen, Germany, 2019.

[8] Stohlman, O. R., Zander, M. E., Fernandez, J. M., “Characterization and Modeling of Large Collapsible Tubular Mast Booms,” in *AIAA Scitech 2021 Forum*, Virtual, 2021.

[9] Zander, M. E., Hillebrandt, M., Sinapius, M., Hühne, C., "Mechanical Characterization of Deployable Thin Shell CFRP Booms for the Cubesat De-Orbit Sail," in *The 66th International Astronautical Congress*, Jerusalem, 2015.

[10] Zander, M. E., Wilken, A., Sinapius, M., and Hühne, C., "Mechanical Testing of Deployable Thin Shell CFRP Booms in Ideal and Realistic Interfaces for the Solar Sail Demonstrator Gossamer-1," in *European Conference of Spacecraft Structures, Materials & Environmental Testing*, Toulouse, France, 2016.

[11] Zander, M., Sinapius, M., and Hühne, C., "Preliminary Experiments for an On-orbit Detection System to Monitor Load and Deflection States of Thin Shell CFRP Booms for the Solar Sail Demonstrator Gossamer-1," in *CNES/ESA/DLR ECSSMET*, Braunschweig, Germany, 2014.

[12] Richter, M., Straubel, M., Fernandez, J. M., Stohlman, O. R., and Wilkie, W. K., "Compact Deployment Control Mechanism for the Deployable Backbone Structure of a 500-m2-class Solar Sail," in *5th International Symposium of Solar Sailing*, Aachen, Germany, 2019.

[13] Richter, M., Hillebrandt, M., and Hühne, C.,"Reduction of Moments Induced on the Coiling Hub of a Boom Deployment Mechanism," *15th ECSSMET*, Noordwijk, The Netherlands, 2016.